Circuits for High-Efficiency Avalanche-Diode Oscillators

W. J. EVANS

Abstract—**This paper describes and analyzes the circuits which have been used successfully for TRAPATT oscillator studies. The results lead to a better understanding of the TRAPATT oscillator and yield a simple model of the oscillator which is useful for circuit design.**

The circuit characteristics of an experimental TRAPATT oscillator are determined from measurements on the circuits and from equivalent circuit model calculations. The following conclusions can be drawn from the analysis. First, the avalanche diode requires sufficient capacitance near the diode to sustain the high-current state required for TRAPATT operation. Secondly, at a distance from the diode corresponding to approximately one half-wavelength at the TRAPATT frequency the transmission line containing the diode should be terminated by a low-pass filter. The function of the filter is to pass the TRAPATT frequency and to provide a shorting plane for the harmonics of that frequency. Finally, on the load side of the filter, tuning for the TRAPATT frequency is required.

The model of the circuit described above suggests a simple explanation of the diode–circuit interaction in a TRAPATT oscillator. Simplified waveforms suggested by the model have been used to calculate power output, efficiency, dc voltage change, and RF impedance for the oscillator. The results agree within a few percent with those obtained for an experimental oscillator. An important conclusion of the analysis is that the high-efficiency operation of avalanche diodes at frequencies in the UHF range can be explained by the TRAPATT theory, even though the trapped-plasma or low-voltage state may last only $\frac{1}{20}$th of the oscillation period.

I. Introduction

A NEW high-efficiency mode of operation using avalanche-diode oscillators has been obtained in silicon diodes by Prager, Chang, and Weisbrod [1] and in germanium by Johnston, Scharfetter, and Bartelink [2]. This mode is characterized by efficient conversion of dc to RF energy (up to 60 percent), operation at frequencies well below the transit-time frequency of operation, and a significant change in the dc operating point when the diode switches into the mode. This paper describes several oscillator circuits which have been used to obtain the high-efficiency or TRAPATT (Trapped Plasma Avalanche Triggered Transit) mode of operation, and suggests a simple model to describe the operation of these oscillators. The next section is a review of the important ideas which describe the TRAPATT mode of operation and were first presented by Sharfetter, Bartelink, Gummel, and Johnston [3]. Section III describes the mechanical and electrical properties of the coaxial circuits used to obtain the TRAPATT mode. The last two sections present a simple model for the oscillator and discuss the conclusions which can be drawn from the model.

Manuscript received July 17, 1969. This paper was presented at the International Microwave Symposium, Dallas, Tex., May 5–7, 1969.

The author is with Bell Telephone Laboratories, Inc., Murray Hill, N. J.

II. The TRAPATT Mode

In order to understand the operation of high-efficiency oscillators, it is necessary to understand what happens when large RF voltage swings exist across an IMPATT diode. Therefore, this section will begin with a review of the large-signal behavior of an IMPATT oscillator.

Fig. 1(a) is a plot of the field profile and carrier densities in an oscillating IMPATT diode at a particular point in time. The profile shown here is for a 6-GHz n^+-p-p^+ epitaxial germanium diode [4]. The plots are made for the particular point in the RF voltage and current waveforms indicated by the squares in Fig. 1(b). The carriers shown have been generated by avalanche breakdown in the high-field region on the left. The holes then drift to the right and the electrons to the left.

One of the saturation mechanisms of this mode of operation is seen in the depression of the field by the space charge of the avalanche-generated carriers. The reduction in field turns off the avalanche prematurely and thus reduces the phase delay provided by the avalanche. This in turn reduces the negative conductance of the oscillator.

Another saturation mechanism is illustrated in Fig. 2. Here the effect of the space charge on the field can be seen after generation has stopped and the holes have drifted into the lower field region of the diode. Again the space charge is depressing the field, so that to the left of the carrier pulse the carrier drift velocity may drop below saturation and some carriers may be trapped for a short time in the low-field region. This change in carrier velocity is not in itself a lossy process as will be seen in the discussion of the TRAPATT mode. However, it does sufficiently change the terminal current waveforms so that the power generated at the transit-time frequency is reduced.

The diode shown in Figs. 1 and 2 will also generate high-efficiency oscillations at frequencies below 3 GHz. However, at the bias current densities used in these oscillators, the diode exhibits no small-signal negative resistance in this frequency range. Therefore in order to start the TRAPATT oscillations, it has been found that very large IMPATT-generated 6-GHz voltage swings must exist across the diode. Thus, in the TRAPATT mode these two saturation mechanisms, i.e., space-charge suppression of the avalanche and carrier trapping, play an important role.

Fig. 3 shows the situation which can occur when the diode shown previously is operated in a high Q circuit where these large RF voltages can develop. The field and carrier densities are shown at a point in time just after the diode voltage has reached a maximum. In this case, the large overdrive in voltage causes the generation of a large amount

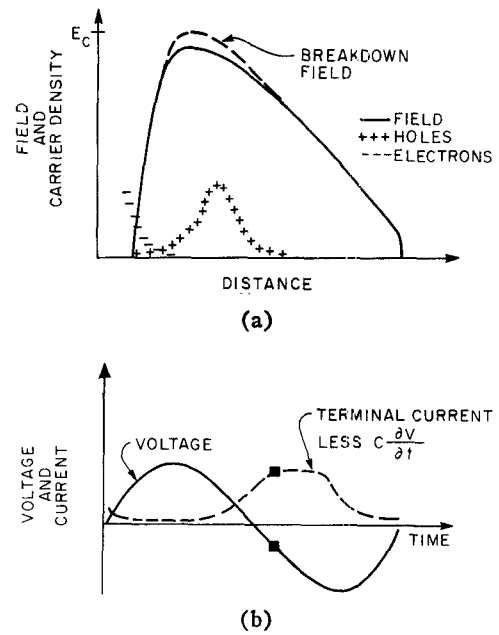

Fig. 1. (a) Large-signal IMPATT field and carrier densities during the avalanche portion of the RF cycle indicated by the squares in (b).

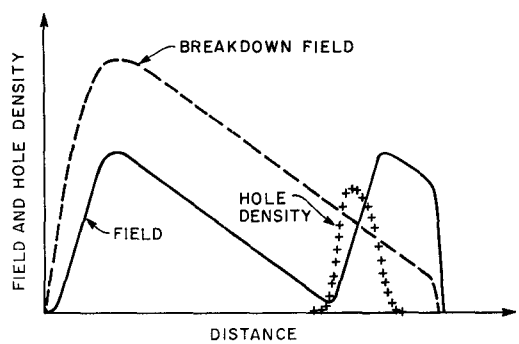

Fig. 2. Large-signal IMPATT field and carrier densities during the drift portion of the RF cycle.

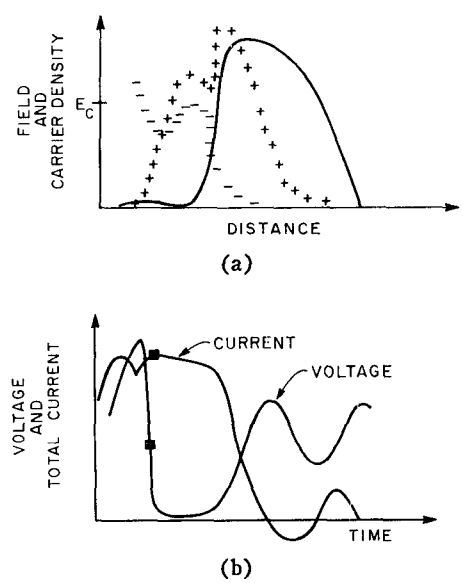

Fig. 3. TRAPATT waveforms. (a) Field and carrier density. (b) Voltage and current.

of charge which is sufficient to reduce the field to nearly zero on the left. However, the field ahead of these carriers is still above the critical field. Thus, an avalanche zone has been created which travels through the diode leaving the diode filled with a plasma of electrons and holes and nearly zero electric field. Because of the low-field condition the plasma is trapped and is extracted at the boundaries by space-charge-limited flow.

The terminal characteristics of this mode for the full cycle are shown in Fig. 3(b). Initially, there is a current which charges the depletion layer capacitance to a voltage of about twice the breakdown voltage. This initiates the traveling avalanche zone which drops the voltage to almost zero. The particle current is very high during this low-voltage state. After the plasma has been removed from the diode, the current drops to a low average value and the voltage returns to near the breakdown value. Therefore this is a very efficient mode of oscillation, which has been calculated to be capable of efficiencies of over 60 percent in silicon and 50 percent in germanium [5].

A final point to be made is that this mode can exist without generating high-efficiency oscillations. In that case, the peak voltage is slightly less, the traveling avalanche does not travel through the complete diode, and it leaves behind only a small amount of trapped charge. Computer-simulated oscillators have shown trapped-plasma states existing for oscillations with less than 1 percent efficiency.

From this description of the operation of the TRAPATT mode, at least one circuit requirement is clear. Namely, in order to obtain self-starting TRAPATT oscillation, large IMPATT-generated voltage swings must be obtained by trapping the IMPATT oscillation in a high-Q cavity.

III. Circuit Description

In this section a short description and analysis of the circuits used to generate TRAPATT oscillation are presented. The typical circuit used in much of the experimental work is shown in Fig. 4. It consists of a coaxial air line with a number of coaxial tuning sleeves and is similar to the IMPATT circuit described by Iglesias [6]. The particular example shown here is the 500-MHz oscillator which generates 5.5 watts of CW power at 43 percent efficiency. The type of circuit has also been used by Johnston [2] to obtain 3-GHz TRAPATT operation under pulse conditions. The large number of tuners in this circuit would be a handicap for some applications; however, the results of the analysis presented here have led to the construction of a very simple circuit using mainly commercial components. That circuit will be described in Section V.

Measurements on the section of line containing the four tuners to the right of plane A-A can easily be made since the line contains a connector pair at that point. Fig. 5 shows the return loss of the section of line containing the four tuners, looking from A-A toward the load. The general characteristic of the circuit, when it is adjusted for high-efficiency operation of the oscillator, is seen to be that of a low-pass filter. Most frequencies above 3 GHz are reflected by the filter formed by the four tuners. The second point to

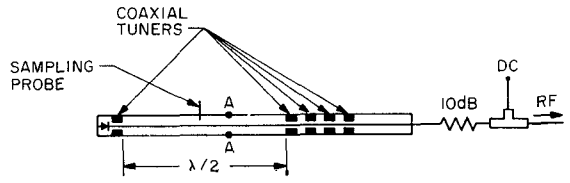

Fig. 4. TRAPATT 500-MHz oscillator circuit.

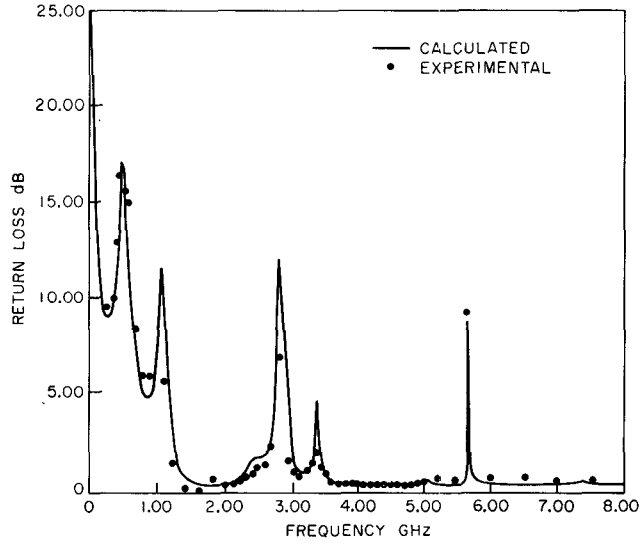

Fig. 5. Return loss versus frequency for the four-slug tuner.

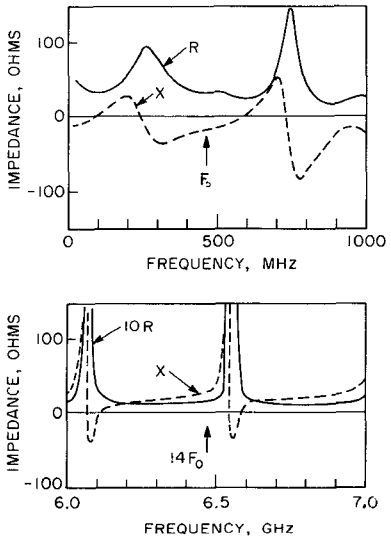

Fig. 6. Circuit impedance at the active terminals of the diode for two frequency ranges.

note is that the circuit matches well to the 50-ohm load at 500 MHz.

Shown also is a calculation of the return loss versus frequency using an equivalent circuit model for the four-slug tuner. The close agreement between these two results indicates that a reasonably accurate calculation of the circuit impedance seen by the active region of the diode can be made by extending the equivalent circuit to the active region of the diode. Fig. 6 shows the results of such a calculation from 0 to 1 GHz and from 6 to 7 GHz. At 460 MHz, the impedance has a substantial real part, about 35 ohms, and a capacitive reactance of 20 ohms. The Q is about 1. In the microwave region, a small part of which is shown, the circuit looks like a shorted transmission line, approximately 30 cm long, which provides a resonance every 500 MHz. At harmonics of the 460-MHz oscillator frequency, the circuit presents a small series resistance (about 2 ohms) to the diode, and a reactance which approximately resonates the diode. The Q at these harmonics is calculated to be about 300 and is consistent with locking range measurements.

IV. Oscillator Model

Next consider the dc operating point for the 500-MHz oscillator. The dc bias current is generally less than 1000 A/cm^2. On the other hand, the conduction current required [5] for the initiation of the trapped plasma in these diodes is 10 000–20 000 A/cm^2. Therefore, since the average value of the conduction current is the dc current, the high-current state exists for less than 0.2 ns. On the other hand, the transit time of the carriers through the diode sets a minimum recovery time from the plasma state of about 0.1 ns. Therefore, TRAPATT operation will occur only if the conduction current consists of pulses of current approximately 0.1 ns in duration occurring once during each cycle of the 500-MHz oscillation.

The conclusion suggests the *diode* model shown in Fig. 7(a). Here, it is assumed that the diode can be represented by a current pulse generator and the diode's depletion layer capacitance. Fig. 7(b) shows the sampling probe used to measure the high-frequency waveforms which are confined to the first section of air line. The transfer function for the current i to the probe voltage v is easily calculated for this circuit, and Fig. 8 shows the results of such a calculation. Here a current pulse of 10 000 A/cm^2, 0.1 ns wide with a period of 2.2 ns has been applied to the circuit. The second plot shows the calculated probe response. The third plot shows a sampling scope photograph of the probe voltage for an operating oscillator. The agreement for such a simple diode model is very good.

These results suggest the following simple interpretation of the operation of the 500-MHz oscillator. The large voltage pulse which passes the probe at A, reaches the diode at B, and triggers the traveling avalanche zone in the diode. This initiates a high-current low-voltage state, from which the diode recovers quickly. The drop in voltage propagates down the line reaching the probe at C. The negative going pulse next reaches the high-frequency short provided by the four-slug tuner where the -1 reflection coefficient causes a positive pulse to be reflected back toward the diode. This pulse passes the probe at A and the process repeats itself.

If this analysis is correct, certain aspects of the oscillator behavior can be predicted. For example, the frequency of operation should be inversely proportional to the length of line between the low-pass filter and the diode. Fig. 9, which gives some measurements on two oscillators, shows this to be the case. The pulsed TRAPATT measurements were

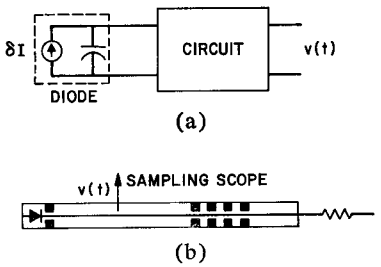

Fig. 7. (a) Simplified diode model. (b) Sampling probe position.

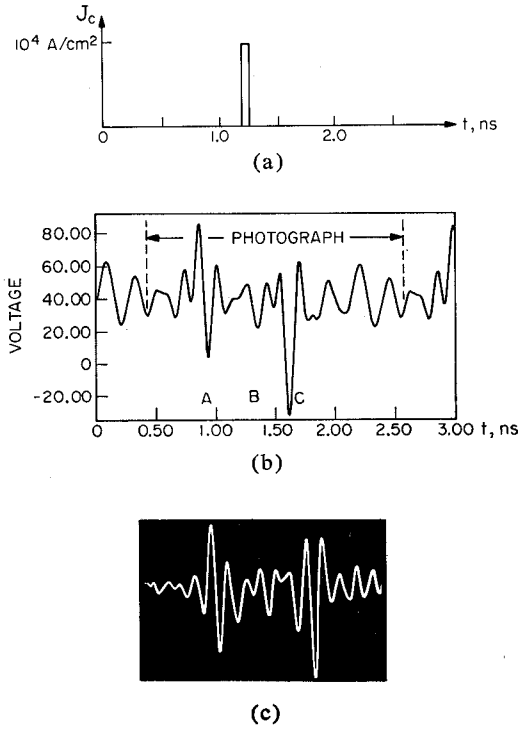

Fig. 8. Probe response. (a) Conduction current versus time. (b) Calculated probe voltage. (c) Measured probe voltage.

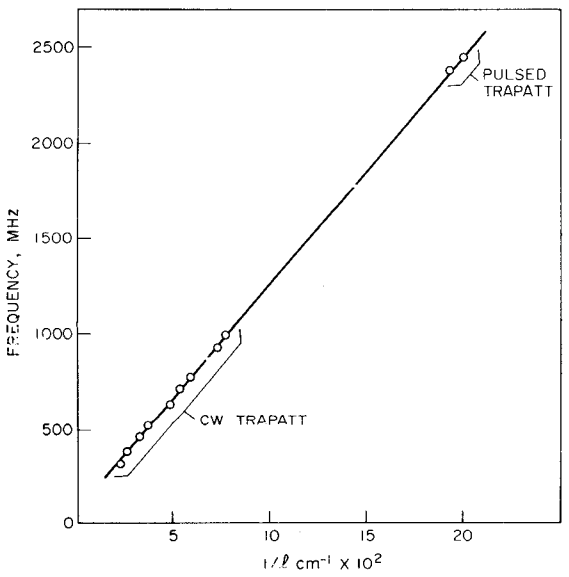

Fig. 9. Oscillator frequency versus filter position.

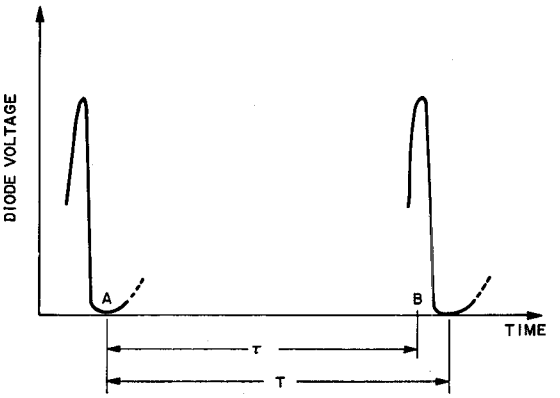

Fig. 10. A portion of the RF voltage waveform for the TRAPATT oscillator.

obtained by R. L. Johnston. The CW TRAPATT results were obtained with the oscillator described previously. Note the rather large tuning range for this CW circuit. Over this range the power output decreases approximately linearly with frequency. If the efficiency is assumed to be unsaturated and the dc current fixed, this linear decrease in power output can be predicted from the simple model presented here. These calculations will be discussed in Section V.

The frequency of operation for these oscillators can be very accurately predicted by measuring the distance between the reflecting plane of the filter and the diode. However, the round-trip delay for the pulse in this length of line does not directly give the period of the oscillation. Fig. 10 shows why this is so. Shown there is a very simplified sketch of the voltage across the diode which triggers the traveling avalanche. Because of the -1 reflection coefficient of the filter, it is the drop in voltage at A which produces the over voltage at B. Therefore, the period of the oscillation must include the time required for the diode voltage to drop to zero. This is typically about 0.1 ns for the germanium diodes used in the experiments described here. Since this is a small fraction of the 2-ns period of the 500-MHz oscillator, the typical value is sufficiently accurate for most calculations. For example, with a cavity length of 30.5 cm, the frequency calculated from only the transmission line delay is 491 MHz. However, if 0.1 ns is added to the total period, the frequency is 468 MHz. The measured frequency was 462 MHz.

It is also possible to construct a general *circuit* model for this mode of operation. Fig. 11 shows such a model. The inductance L is the usual diode lead inductance; its size is not critical, but it is helpful in driving the diode voltage to more than twice breakdown to initiate the TRAPATT plasma state. The next element is a capacitance. A calculation of the current required by the diode in the high-current state shows that a 50-ohm line is not able to supply the required current. Therefore, a lumped capacitance is required at this point. Next is a length of transmission line whose length determines the operating frequency. This line is terminated in a low-pass filter which appears to be a short circuit at frequencies above the cutoff. Finally, a tuner is needed to match the diode to the load.

This representation of the coaxial circuit is very simple,

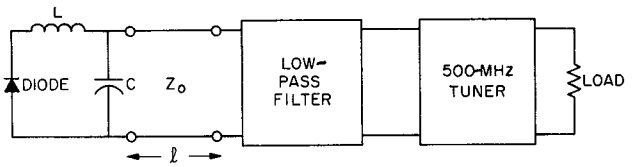

Fig. 11. Simplified TRAPATT circuit model.

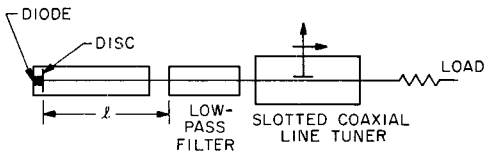

Fig. 12. Simplified TRAPATT circuit.

TABLE I

EXPERIMENTAL DATA FOR CIRCUIT SHOWN IN FIG. 12

Low-Pass Filter Cutoff	Power at 500 MHz (watts)	Power at 1000 MHz (watts)
700 MHz	2.7	—
1000 MHz	1.7	—
1500 MHz	2.5	1.4
3000 MHz	1.3	1.0
4000 MHz	0.9	0.9
4-slug filter	2.6	1.3

I_{dc}=200 mA.

but Fig. 12 shows that this is all that is required. Shown is a simple circuit which is very useful for laboratory measurements. It consists of a coaxial air line with the diode mounted in one end. Contacting the diode package is a 1-pF lumped capacitor formed by a disk on the center conductor. A distance down the line is a commercial low-pass filter. Following the low-pass filter is a commercial slotted coaxial line tuner. The experimental results for such an oscillator are shown in Table I. Notice that generally speaking, as fewer harmonics of the TRAPATT oscillation are confined to the high-Q cavity, the shape of the pulse reflected by the filter is degraded, and the power output decreases.

With a slight retuning of the circuit, 1-GHz oscillations are excited. In that case the cavity is twice as long as it need be, so that two pulses are on the line at the same time. This circuit has also been used to build a high-efficiency 500-MHz CW amplifier by placing a circulator at the load terminals.

V. Low-Frequency Waveforms

In the last section a simple model of the diode and the circuit for a TRAPATT oscillator were discussed. In this section the model will be expanded so that calculations on oscillator efficiency can be made in terms of some circuit parameters.

It was pointed out above that the conduction current for a 500-MHz oscillator is very large but flows for only a short period of time. Therefore, charge which flows through the diode for this short period of time must come from the

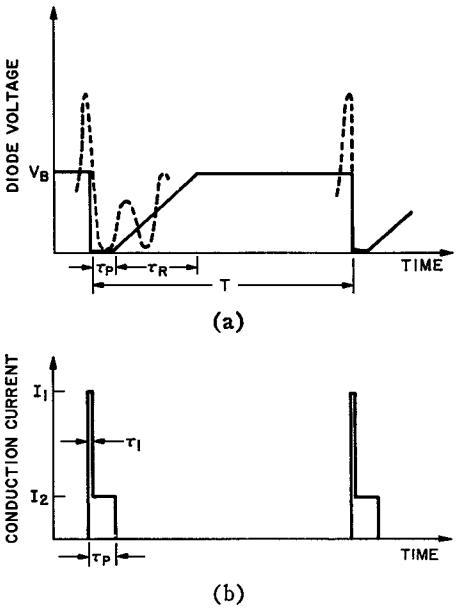

Fig. 13. TRAPATT voltage (a) and current (b) waveforms.

capacitance in the immediate vicinity of the diode.[1] The capacitance which can be discharged during that time consists of the lumped capacitance near the diode and the capacitance of a length of line which depends on the duration of the high-current state.[2] Therefore, the total capacitance can be written as

$$C_T = C_0 + \tau_P/Z_0 \tag{1}$$

where

C_0=the lumped capacitance near the diode,
τ_p=the length of time that the high-current or trapped-plasma state exists,
Z_0=the characteristic impedance of the coaxial air line.

After the plasma has been cleared from the diode, the diode voltage is nearly back to its breakdown value. However, the capacitance near the diode can recover only as quickly as the line can recharge it. The diode voltage will thus have a shape similar to that shown by the broken line in Fig. 13(a). The sinusoidal variations shown there are due to ringing of the circuit inductance and capacitance near the diode. To a first approximation, it will be assumed that the average value of the voltage near the diode increases linearly after the high-current state and stops when it reaches the breakdown voltage. This is a reasonable assumption since the capacitance near the diode is recharged by a transmission line. For this model the conduction current will have the shape shown in Fig. 13(b). Initially a large current flows which discharges the lumped capacitance near the diode. This is followed by a lower current which discharges a short length of the transmission line. This type of current waveform has been found in computer simulations of a 500-MHz

[1] In some oscillators this may be present in the form of an RF bypass capacitor in the dc bias connection.

[2] In this regard the oscillator operates very much like the relaxation oscillation analyzed by Ward and Udelson [7].

oscillator. If there is no lumped capacitance near the diode (in this case the diode area is reduced so that the transmission line can supply the required current density) the current waveform is approximately rectangular [5].

Neglecting the initial spike of voltage which initiates the traveling avalanche, the amplitudes of the fundamental components of voltage and current, shown by the solid lines in Fig. 13, are

$$V_{ac} = \frac{V_B}{\pi}\left\{\frac{\cos\omega(\tau_R+\tau_P)-\cos\omega\tau_P}{\omega\tau_R} + j\left(1-\frac{\sin\omega(\tau_R+\tau_P)-\sin\omega\tau_P}{\omega\tau_R}\right)\right\} \quad (2)$$

and since $\omega\tau_1 \ll 1$,

$$I_{ac} \simeq \frac{I_1\omega\tau_1}{\pi} + \frac{I_2}{\pi}\{\sin\omega\tau_P + j(\cos\omega\tau_P - 1)\}. \quad (3)$$

The power and impedance at the fundamental frequency are given by[3]

$$P = \tfrac{1}{2}\,\mathrm{Re}(I_{ac}\cdot V_{ac}) \quad (4)$$

$$Z = V_{ac}/I_{ac}. \quad (5)$$

The recovery time τ_R is estimated by assuming a constant charging current during the recovery and is given by

$$\tau_R \simeq Z_0 C_T. \quad (6)$$

The dc current is given by

$$I_{dc} = \frac{Q}{T} = \frac{I_1\tau_1}{T} + \frac{I_2\tau_P}{T} \quad (7)$$

where

$$\omega = 2\pi/T.$$

The charge $I_1\tau_1$ comes from the lumped capacitor C_0 which is charged to approximately $2V_B$ (by the triggering pulse). Therefore,

$$I_1\tau_1 = 2V_BC_0. \quad (8)$$

The charge $I_2\tau_p$ comes from the transmission line which is charged to about V_B. Therefore,

$$I_2\tau_P = \frac{V_B}{Z_0}\tau_P. \quad (9)$$

Equation (7) can therefore be written as

$$I_{ac} = \frac{I_{dc}}{\pi}\left\{\frac{2\pi\gamma}{1+\gamma} + \frac{1}{1+\gamma}\cdot\frac{T}{\tau_P}(\sin\omega\tau_P + j(\cos\omega\tau_P - 1))\right\} \quad (10)$$

where

[3] The actual recovery would be approximately exponential, but the linear approximation is adequate for this discussion.

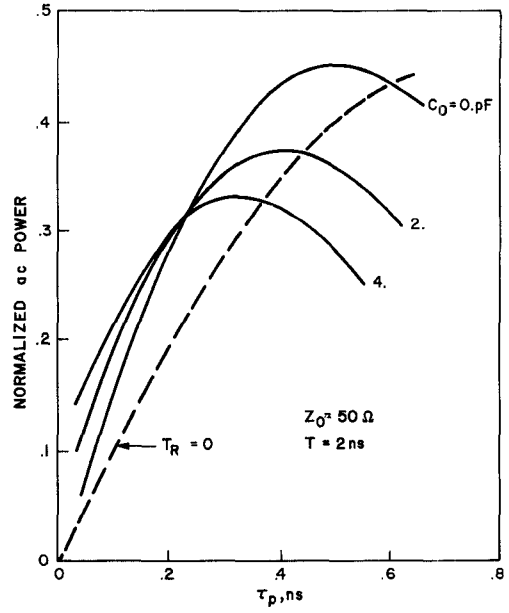

Fig. 14. Ac power versus trapped-plasma duration τ_P for several values of the lumped capacitance C_0.

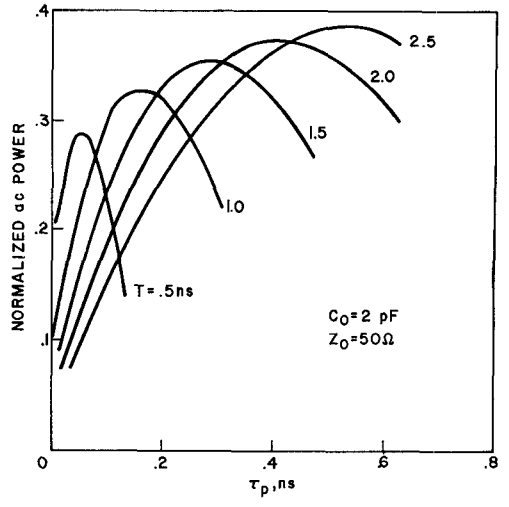

Fig. 15. Ac power versus trapped-plasma duration τ_P for several oscillator frequencies.

$$\gamma = 2C_0Z_0/\tau_P.$$

Although this is a simple model of the oscillator it does yield some interesting results. Fig. 14 shows the ac power output (normalized to $I_{dc}V_B$) for a 500-MHz oscillator with a 50-ohm line and various values of lumped capacitance near the diode. The broken curve is for the case in which the recovery time is neglected, i.e., the voltage recovers instantly after the trapped-plasma state. The figure shows that, for high-current states of short duration, the recharging part of the cycle is instrumental in producing high-efficiency oscillation. For a trapped plasma lasting about 0.1 ns, this increase in ac power is more than a factor of 2 for a lumped capacitance of 4 pF.

Fig. 15 shows the normalized ac power output as a function of τ_P with the oscillator period as a parameter. Using

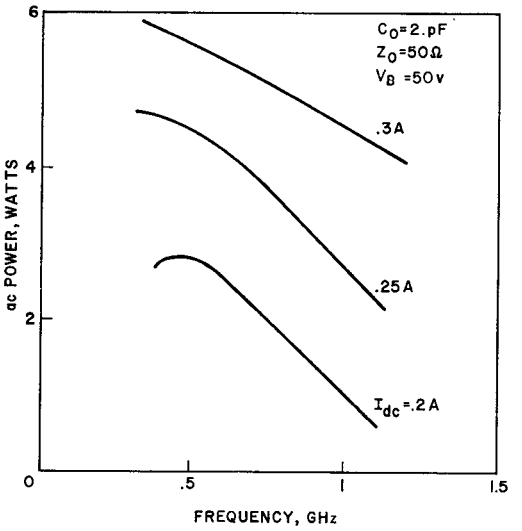

Fig. 16. Ac power versus frequency for values of dc bias current.

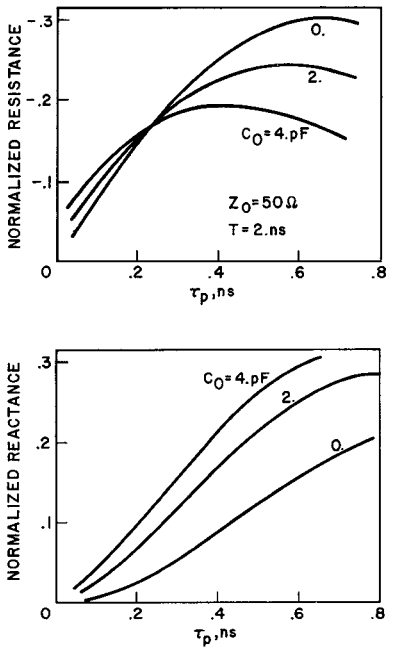

Fig. 17. Diode impedance versus trapped-plasma duration τ_P for several values of the lumped capacitance C_0.

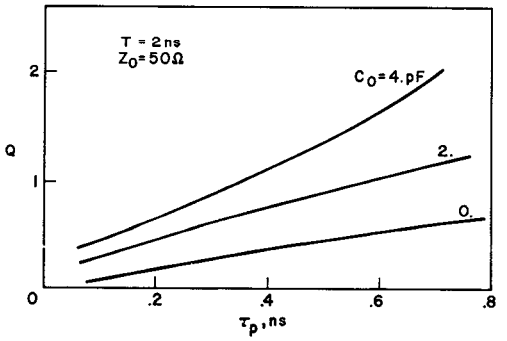

Fig. 18. Diode Q (reactance/resistance) versus trapped plasma duration τ_P.

TABLE II

	Calculation	Experimental
ac power (watts)	2.5	2.6
dc voltage (volts)	41.5	38.9
Efficiency (percent)	30	34
Diode resistance (ohms)	−33.7	−35.5
Diode reactance (ohms)	16.7	19.0

these curves and assuming a diode with a breakdown voltage of 50 volts, the power output as a function of frequency for various bias currents is obtained and is shown in Fig. 16. As mentioned previously, the decrease in power with frequency has been observed experimentally. The normalized diode impedance (normalized to V_B/I_{dc}) is shown in Fig. 17. These results will be used in a specified example given below. The diode Q (the ratio of reactance to resistance) is shown in Fig. 18. The Q is seen to be quite low for most values of τ_P and C_0.

For the 500-MHz oscillator considered in Section IV, the total lumped capacitance near the diode is about 2.8 pF. Using (7)–(9), τ_P is given by

$$\tau_P = \left(\frac{TI_{dc}}{V_B} - 2C_0\right) Z_0. \tag{11}$$

With a diode breakdown voltage of 50 volts and a dc current of 200 mA, τ_P is found to be about 0.17 ns. Using this value of τ_P, the operating point for the oscillator can be found from Figs. 14 and 17. The calculated values are compared with an experimental oscillator in Table II.

The dc voltage is calculated from the voltage waveform shown in Fig. 13. The dc power is the product of this voltage and the dc current. However, the waveforms shown in Fig. 13 do not allow any power dissipation, so that the dc power in excess of that converted to 500-MHz energy must be in the harmonics. However, in the experimental oscillator, the harmonics are reactively terminated so that they do not dissipate power. This situation can be achieved with the waveforms shown by assuming the current pulse begins just after the triggering voltage and requiring the voltage to drop with a finite slope. This is found to make the higher harmonics almost purely reactive while having little effect at the fundamental. The power dissipated in driving the avalanche through a diode is then

$$P_{av} \simeq V_B \cdot I_1 \frac{\tau_1}{T}$$

where τ_1 is the time required for the avalanche to sweep through the diode. This result follows if we assume that, for the transmission-line type of oscillator discussed here, the peak diode voltage is about $2V_B$.

Bartelink and Scharfetter [8] have shown that the velocity with which the avalanche sweeps through the diode is

$$v = \frac{I_1}{qN_a}$$

where N_a is the impurity concentration for a uniformly doped depletion region. Therefore,

$$P_{av} \simeq V_B \frac{qN_a}{T} l$$

where l is the depletion layer width. In a similar way the waveforms could be modified to include the energy required to remove carriers from the diode. For oscillators which have some lumped capacitance near the diode, the current at the end of the trapped-plasma state is small (at the time when the voltage is increasing), and therefore the energy lost during this part of the cycle may be rather small. For a more complete discussion of the energy-loss mechanisms in these oscillators the reader is referred to a paper by DeLoach and Scharfetter [9].

Equation (11) used above to calculate τ_P has some other interesting consequences. Since τ_P must be at least as large as the transit time of carriers through the diode, this puts an upper limit on the lumped capacitance C_0. On the other hand, for large-area diodes, a great deal of terminal current is required initially to drive the avalanche zone through the diode. This in turn requires a large value of C_0. Equation (11) also gives a useful relation between frequency, dc current, and breakdown voltage. In fact, even though the analysis does not appear to contain any material parameters, the equation predicts a substantial difference between germanium and silicon diodes. For example, to obtain results comparable to the germanium oscillator discussed above in a silicon diode with a breakdown voltage of 100 volts required about 0.4 ampere, or twice that used in germanium. (This is four times the power density and requires pulsed operation.) It should be noted also that the impedance of germanium and silicon diodes is the same in this case since the normalizing factor for Z is V_B/I_{dc}. Finally, since the minimum τ_P is fixed for a given diode, the dc current must increase with frequency to maintain the efficiency. If τ_P is greater than the minimum, however, the current need not be strictly inversely proportional to T.

VI. Conclusions

In Section IV the circuit conditions required to initiate the trapped-plasma state and sustain oscillation were discussed. In particular it was found that higher order harmonics must be trapped in order to sustain a voltage pulse which initiates the traveling avalanche. The frequency was found to be controlled by the transit time of this pulse between the diode and the low-pass filter. Finally a simple circuit was presented which was suggested by the analysis and is very useful for laboratory work.

In Section V the low-frequency characteristics of the waveform were examined in order to determine the circuit conditions required for high-efficiency operation. It was found that the time required to recharge the capacitance near the diode after the trapped-plasma state has a significant effect on the oscillator efficiency. In particular, it is found that high-efficiency oscillations are possible even though the trapped-plasma state lasts only a small fraction of the total period (e.g., $\frac{1}{20}$). This occurs because the circuit recovery time is much longer than the diode recovery time. It was also shown that the dc power requirements for silicon and germanium are somewhat different.

The simple model of TRAPATT oscillators which has been presented here is very useful for circuit design and performance calculations. However, very little has been said about the diode design. The analysis assumes that a trapped-plasma state can be excited and that the diode will generate sufficient power in the harmonics to make up for circuit losses, and regenerate the required voltage pulse.

Acknowledgment

The author would like to acknowledge the contributions of D. L. Scharfetter to this paper and helpful discussions with B. C. DeLoach, R. L. Johnston, and D. E. Iglesias.

References

[1] H. J. Prager, K. K. N. Chang, and S. Weisbrod, "High power, high efficiency silicon avalanche diodes at ultra high frequencies," *Proc. IEEE* (Letters), vol. 55, pp. 586–587, April 1967.
[2] R. L. Johnston, D. L. Scharfetter, and D. J. Bartelink, "High-efficiency oscillations in Ge avalanche diodes below the transit-time frequency," *Proc. IEEE* (Letters), vol. 56, pp. 1611–1613, September 1968.
[3] D. L. Scharfetter, D. J. Bartelink, H. K. Gummel, and R. L. Johnston, "Computer simulation of low frequency high efficiency oscillation in germanium," presented at the IEEE Solid State Device Research Conference, June 17–19, 1968.
[4] R. L. Rulison, G. Gibbons, and J. G. Josenhans, "Improved performance of IMPATT diodes fabricated from germanium," *Proc. IEEE* (Letters), vol. 55, pp. 223–224, February 1967.
[5] D. L. Scharfetter, "Power-frequency characteristics of the TRAPATT diode mode of high efficiency power generation in germanium and silicon avalanche diodes," presented at the IEEE Device Research Conference, Rochester, N. Y., June 23–26, 1969.
[6] D. E. Iglesias, "Circuit for testing in high-efficiency IMPATT diodes," *Proc. IEEE* (Letters), vol. 55, pp. 2065–2066, November 1967.
[7] A. L. Ward and B. J. Udelson, "Computer calculation of avalanche-induced relaxation oscillations in silicon diodes," *IEEE Trans. Electron Devices*, vol. ED-15, pp. 847–851, November 1968.
[8] D. J. Bartelink and D. L. Scharfetter, "Avalanche shock fronts in p-n junctions," *Appl. Phys. Letters*, May 15, 1969.
[9] B. C. De Loach, Jr., and D. L. Scharfetter, "Device physics of TRAPATT oscillators," to be published.